LAWRENCE
LIVERMORE
NATIONAL
LABORATORY

LLNL-CONF-649613

Efficient and Accurate Correction of Beam Hardening Artifacts

K. M. Champley, T. Bremer

February 10, 2014

The Third International Conference on Image Formation in X-Ray Computed Tomography
Salt Lake City, UT, United States
June 22, 2014 through June 25, 2014

Disclaimer

Efficient and Accurate Correction of Beam Hardening Artifacts

Kyle Champley and Timo Bremer

***Abstract*—The polychromatic energy-spectra of X-ray tubes used in Computed Tomography (CT) produce so-called *beam hardening* artifacts in the reconstructed images. These artifacts diminish the quantitative accuracy and qualitative appearance of the CT images. Modern model-based beam hardening correction (BHC) algorithms are effective at removing these artifacts, but are extremely computationally expensive. In this paper we develop a new model-based BHC algorithm that is both effective and computationally efficient. The method consists of two nested loops. The outer loop estimates the energy dependence on the measured ray-sums of the attenuation map and the inner loop determines the sinogram data that fits the energy-weighted forward model of CT data.**

I. Introduction

X-ray Computed Tomography (CT) allows one to non-destructively obtain images of the structural makeup of an object of interest. A number of physical effects in the measured data may diminish the qualitative and quantitative accuracy of the image. This paper deals with the correction of so-called *beam-hardening* artifacts.

The attenuation of a monochromatic X-ray beam through a uniform object is given by $-\log(I/I_0) = \mu l$, where I_0 and I are the intensity of the beam before and after the beam travels through the object, μ is the attenuation coefficient (at the given energy of the beam), and l is the path-length through the object.

The relationship between the attenuation of a polychromatic X-ray beam through an object and the attenuation map is highly nonlinear. The rate of absorption and scattering of X-rays depends on the X-ray energy and the material composition. Lower energy X-rays are absorbed at a higher rate which causes the beam to *harden*. The violation of the assumed linear relationship between the measurements and the object attenuation map by the polychromatic X-ray CT spectra introduces *beam hardening* artifacts into the reconstructed CT images.

Methods for beam hardening correction (BHC) have been developed over the past several decades[1], [2], [3], [4], [5], [6], [7], [8] to mitigate beam hardening artifacts. Earlier approaches [1], [2], [3], [4] may be categorized as post-reconstruction techniques. These methods are computationally efficient, but not as accurate as state-of-theart model based iterative methods [5], [6], [8] which are computationally intensive.

In this paper we introduce a new computationally-efficient and quantitatively accurate model-based BHC algorithm. We test our algorithm with simulated and measured data and compare its performance with a BHC algorithm developed by Fuchs [3].

The authors are with Lawrence Livermore National Laboratory, Livermore, CA. Corresponding author: Kyle Champley (champley1@llnl.gov)

II. X-ray CT Model

Let γ be the X-ray energy (keV), $d(\gamma)$ be the energy-dependent detector response, and $s(\gamma, L)$ be the source spectra that depends on a particular ray-path, L. Assuming that no scattered radiation is measured by the detectors, the expectation of a radiograph can be modeled by

$$I(L) \quad := \quad \int d(\gamma) s(\gamma, L) e^{-\int_L \mu(\gamma, \mathbf{x})\, d\mathbf{x}}\, d\gamma,$$

where $\mu(\gamma, \mathbf{x})$ cm^{-1} is the energy-dependent attenuation map of the object being scanned and $\mathbf{x} \in \mathbb{R}^3$ is a location in space. Define the *air scan* as the radiograph with the object removed from the field of view. Then its expectation is given by

$$I_0(L) \quad := \quad \int d(\gamma) s(\gamma, L)\, d\gamma.$$

The normalized radiograph is given by

$$\begin{aligned} \frac{I(L)}{I_0(L)} \quad &= \quad \int \widehat{m}(\gamma, L) e^{-\int_L \mu(\gamma, \mathbf{x})\, d\mathbf{x}}\, d\gamma, \\ \widehat{m}(\gamma, L) \quad &:= \quad \frac{d(\gamma) s(\gamma, L)}{\int d(\gamma) s(\gamma, L)\, d\gamma}. \end{aligned}$$

The attenuation map can be reconstructed (with beam-hardening artifacts) from a *sinogram* which is given by

$$p(L) \quad := \quad -\log\left(\frac{I(L)}{I_0(L)}\right) \approx P\mu(\overline{\gamma}, L) \qquad (1)$$

$$P\mu(\overline{\gamma}, L) \quad := \quad \int_L \mu(\overline{\gamma}, \mathbf{x})\, d\mathbf{x}, \qquad (2)$$

where P is the forward projection operator and $\overline{\gamma} = \int \gamma \widehat{m}(\gamma)\, d\gamma$ is the mean effective energy of the system. Equation (2) is only exact for $\widehat{m}(\gamma, L) = \delta(\gamma - \overline{\gamma})$, where $\delta(\cdot)$ is the dirac delta functional.

A. Energy-Dependent Attenuation of Compounds

The attenuation coefficient of a material can be broken up in components of electron density (electrons mol / cm^3) and cross section (cm^2 mol^{-1}/electrons). The absorption and scattering cross section of a material depends on its effective atomic number (also called effective-Z), i.e.,

$$\mu(\gamma, \mathbf{x}) \quad = \quad \sigma(\gamma, Z(\mathbf{x}))\rho(\mathbf{x}),$$

where σ is the cross section, ρ is the density, and $Z(\mathbf{x})$ is the spatially-variant effective-Z map. The photon energy-dependent absorption and scattering cross section for the elements can be found in tables [9]. We shall denote these quantities by $\sigma(\gamma, Z)$ where $Z \in \mathbb{Z}$ is the atomic number of the element. The cross sections of the elements can be extended to non-integer Z by linear interpolation.

These energy-dependent attenuation coefficients can be approximated by the Compton-Photoelectric basis given by

$$\begin{aligned}
\mu(\gamma, \mathbf{x}) &\approx b_c(\gamma) f_c(\mathbf{x}) + b_p(\gamma) f_p(\mathbf{x}) \\
b_c(\gamma) &:= 2\pi r_0^2 N_A \\
&\times \left\{ \frac{1+\alpha}{\alpha^2} \left[\frac{2(1+\alpha)}{1+2\alpha} - \frac{1}{\alpha} \log(1+2\alpha) \right] \right. \\
&+ \left. \frac{1}{2\alpha} \log(1+2\alpha) - \frac{1+3\alpha}{(1+2\alpha)^2} \right\} \frac{\text{mol}^{-1}\text{cm}^2}{\text{electron}} \\
b_p(\gamma) &:= \gamma^{-3},
\end{aligned}$$

where r_0 is the classical electron radius and N_A is Avogadro's number.

Now consider the attenuation maps f_1 and f_2 at the two energies γ_1 and γ_2. Then there exists f_p and f_c such that

$$\begin{aligned}
f_1 &= b_c(\gamma_1) f_c + b_p(\gamma_1) f_p \\
f_2 &= b_c(\gamma_2) f_c + b_p(\gamma_2) f_p
\end{aligned}$$

and conversely

$$\begin{aligned}
f_c &= b_1(\gamma_1) f_1 + b_2(\gamma_1) f_2 \\
f_p &= b_1(\gamma_2) f_1 + b_2(\gamma_2) f_2,
\end{aligned}$$

where

$$b_1(\gamma) := \frac{b_p(\gamma_2) b_c(\gamma) - b_c(\gamma_2) b_p(\gamma)}{b_p(\gamma_2) b_c(\gamma_1) - b_c(\gamma_2) b_p(\gamma_1)} \tag{3}$$

$$b_2(\gamma) := \frac{b_c(\gamma_1) b_p(\gamma) - b_p(\gamma_1) b_c(\gamma)}{b_c(\gamma_1) b_p(\gamma_2) - b_p(\gamma_1) b_c(\gamma_2)} \tag{4}$$

and thus

$$\mu(\gamma, \mathbf{x}) \approx b_1(\gamma) f_1(\mathbf{x}) + b_2(\gamma) f_2(\mathbf{x}).$$

III. Development of Beam Hardening Correction Algorithm

We wish to determine $p := Pf$, where f is the attenuation map at energy $\overline{\gamma}$. Assume that the energy-dependent attenuation map, μ, can be broken up into a finite number of material components by

$$\mu(\gamma, \mathbf{x}) = \sum_{i=1}^{M} \widehat{\sigma}_i(\gamma) a_i(\mathbf{x}),$$

where $\widehat{\sigma}_i(\gamma) = \frac{\sigma(\gamma, Z_i)}{\sigma(\overline{\gamma}, Z_i)}$ is the normalized cross section (unit less) of the materials with effective-Z of Z_i and $a_i(\mathbf{x})$ are spatially-dependent attenuation maps (at $\overline{\gamma}$) for each material. Note that this model allows the attenuation map to fluctuate (by variable density) for a given material. The choice of $\{Z_i\}_{i=1}^M$ should be such that different materials can be reasonably determined by either a priori knowledge of the object being scanned or by applying a set of parametric transfer functions to f such as $a_i(\mathbf{x}) := T_i(f)(\mathbf{x})$, where

$$T_i(f)(\mathbf{x}) := \begin{cases} f(\mathbf{x}), & f(\mathbf{x}) < \mu_1, \\ \frac{\mu_i - f(\mathbf{x})}{\mu_i - \mu_{i-1}} \mu_{i-1}, & \mu_{i-1} \le f(\mathbf{x}) < \mu_i, \\ \frac{f(\mathbf{x}) - \mu_i}{\mu_{i+1} - \mu_i} \mu_i, & \mu_i \le f(\mathbf{x}) < \mu_{i+1}, \\ f(\mathbf{x}), & \mu_M < f(\mathbf{x}), \\ 0, & \text{otherwise.} \end{cases} \tag{5}$$

Note that $f = \sum_i a_i$ and μ_i are the attenuation coefficients of our basis elements at the mean effective energy. Other transfer functions may be used, but are not discussed in this paper.

Using the above we can separate the spectra effects of $P\mu(\gamma, L)$ from its value at the mean energy by

$$\begin{aligned}
P\mu(\gamma, L) &= \frac{P\mu(\gamma, L)}{P\mu(\overline{\gamma}, L)} P\mu(\overline{\gamma}, L) \\
&= \frac{\sum_{i=1}^M \widehat{\sigma}_i(\gamma) Pa_i(L)}{\sum_{i=1}^M \widehat{\sigma}_i(\overline{\gamma}) Pa_i(L)} Pf(L) \\
&= \sum_{i=1}^M \widehat{\sigma}_i(\gamma) \frac{Pa_i(L)}{\sum_{j=1}^M Pa_j(L)} Pf(L) \\
&=: c(\gamma, L) p(L).
\end{aligned} \tag{6}$$

This method requires M forward projections to estimate $c(\gamma, L)$. We now show how one can estimate $c(\gamma, L)$ with only one forward projection using equations (3, 4). Now consider the two energies $\overline{\gamma}$ and γ_{peak}, where γ_{peak} is the peak energy of the spectra. Then using equations (3, 4), we may define basis functions $b_{mean}(\gamma)$ and $b_{peak}(\gamma)$ such that

$$\mu(\gamma, \mathbf{x}) \approx b_{mean}(\gamma) f(\mathbf{x}) + b_{peak}(\gamma) f_{peak}(\mathbf{x}).$$

Then using a similar argument as above we find

$$\begin{aligned}
P\mu(\gamma, L) &\approx \left[b_{mean}(\gamma) + b_{peak}(\gamma) \frac{Pf_{peak}(L)}{Pf(L)} \right] Pf(L) \\
&=: c(\gamma, L) Pf(L),
\end{aligned} \tag{7}$$

where $f_{peak}(\mathbf{x}) := \sum_{i=1}^M \widehat{\sigma}_i(\gamma_{peak}) a_i(\mathbf{x})$.

IV. Iterative Estimation of Model Parameters

In this section we describe how to iteratively determine the beam hardening model parameters, $c(\gamma, L)$ and in turn the beam hardening corrected sonogram data, $p(L)$.

Suppose that the effective atomic number of the material with the lowest effective atomic number in the model is given by Z_1. For example, in medical CT $Z_1 = 7.42$, the effective atomic number of water. Also let A be the filtered backprojection (FBP) operator. Then our algorithm is given by

1) Initialize $n = 0$ and $p_{0,0} := -\log\left(\frac{I}{I_0}\right)$
2) Set $c_n(\gamma)$:

$$\begin{aligned}
c_n(\gamma) &:= \begin{cases} \widehat{\sigma}_1(\gamma), & n = 0, \\ b_{mean}(\gamma) + b_{peak}(\gamma) \frac{Pf_{n,peak}}{p_{n,0}}, & n \ge 1 \end{cases} \\
f_n &:= A p_{n,0}, \qquad n \ge 1 \\
f_{n,peak} &:= \sum_{i=1}^M \widehat{\sigma}_i(\gamma_{peak}) T_i(f_n), \qquad n \ge 1
\end{aligned}$$

3) Use Newton's Method to find sinogram data that matches polychromatic model (for $k = 0, 1, \ldots, K-1$):

$$p_{n,k+1} := p_{n,k} + \frac{\int \widehat{m}(\gamma) e^{-p_{n,k} c_n(\gamma)}\, d\gamma}{\int c_n(\gamma) \widehat{m}(\gamma) e^{-p_{n,k} c_n(\gamma)}\, d\gamma} \times \left[\log\left(\int \widehat{m}(\gamma) e^{-p_{n,k} c_n(\gamma)}\, d\gamma \right) + p_{0,0} \right]$$

4) Update beam corrected sinogram: $p_{n+1,0} := p_{n,K-1}$
5) Increment n and repeat steps 2 through 4

For notational simplicity we have dropped the arguments of L from the above equations.

Thus the inner loop (in k) uses Newton's method to determine the best match between the measured data and the polychromatic forward model of the data. This model requires knowledge of $c(\gamma, L)$ which is iteratively estimated in the outer loop (in n) of the algorithm.

Note that the first iteration (in n) of the algorithm does not require a reconstruction and the first image reconstructed has already been partially corrected for beam hardening artifacts.

V. Methods

We tested our algorithm on both simulated and measured data from an Imatron electron-beam CT (EBCT) scanner. The spectra and detector response of the measured data are unknown; we only know that the spectra has a peak energy of 130 keV. We modeled this spectra using the techniques proposed in [10]. Using this spectra model and uniform detector response, i.e., $d(\gamma) = 1$, the mean effective energy of the system is estimated to be $\overline{\gamma} = 61.27$. We partitioned our BHC model into three components: water, aluminum, and titanium.

To provide a basis for comparison, we also implemented a BHC method developed by Fuchs [3]. The method is given by

$$\begin{aligned} p_0 &:= -\log(I/I_0) \\ p_1 &:= 2p_0 + \log\left(\int \widehat{m}(\gamma) e^{-\widehat{\sigma}_i(\gamma) p_0}\, d\gamma \right) \\ g_{n,i} &:= PT_i(f_n) \\ p_{n+1} &:= p_0 + \sum_{i=1}^{M} g_{n,i} \\ &\quad + \log\left(\int \widehat{m}(\gamma) e^{-\sum_{i=1}^{M} \widehat{\sigma}_i(\gamma) g_{n,i}}\, d\gamma \right). \end{aligned}$$

The Fuchs algorithm shares some similarities with our algorithm. In our algorithm, the forward model of the corrected data essentially matches the measured data. This is not true for the Fuchs algorithm.

A list of attenuation coefficients and effective-Z of the materials used in our simulations is shown in Table I. The FBP reconstruction of the phantoms used in our simulations are shown in Figure 1. We simulated 500 views (over 180°) of parallel-beam data with 512 rays per view using analytic ray-tracing techniques and a polychromatic spectra with peak energy of 130 keV. Noise was not included in the simulation so we could isolate the beam hardening artifact and correction.

The Imatron CT data is comprised of a single-row of fan beam projections with 888 views (over 222°) and 864 rays per view. Multiple axial slices were taken in step-and-shoot mode.

TABLE I
Material Properties

material	electron density	Z	attenuation	HU
graphite	0.9012 $\frac{\text{electrons mol}}{\text{cm}^3}$	6	0.3140 cm^{-1}	1542
water	0.554 $\frac{\text{electrons mol}}{\text{cm}^3}$	7.42	0.2040 cm^{-1}	1000
magnesium	0.8610 $\frac{\text{electrons mol}}{\text{cm}^3}$	12	0.4370 cm^{-1}	2147
aluminum	1.3009 $\frac{\text{electrons mol}}{\text{cm}^3}$	13	0.7290 cm^{-1}	3581
silicon	1.1580 $\frac{\text{electrons mol}}{\text{cm}^3}$	14	0.7210 cm^{-1}	3543
titanium	2.0710 $\frac{\text{electrons mol}}{\text{cm}^3}$	22	3.2820 cm^{-1}	16121

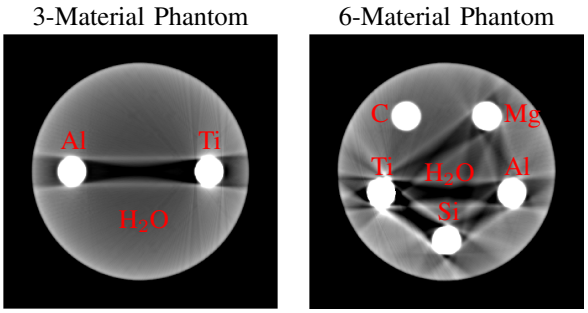

Fig. 1. FBP Reconstructions. Window: [900 1100] HU.

VI. Results

Results are shown in Figures 2, 3, 4, and 5.

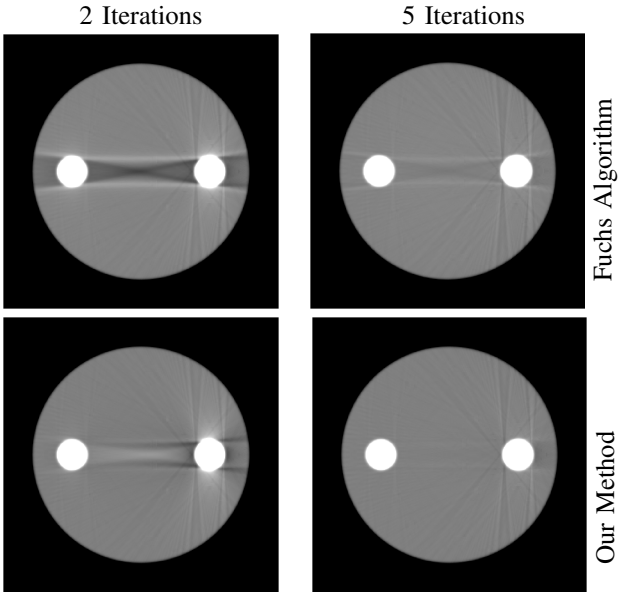

Fig. 2. Reconstructed images are the 3-material phantom. Window: [900, 1100] HU.

VII. Discussion and Conclusion

In this paper we have developed and tested an efficient and accurate model-based beam hardening correction algorithm for X-ray CT. Experiments show that the algorithm effectively converged in five iterations, removing streaks and improving quantification. Our algorithm seemed to converge significantly faster than the algorithm developed by Fuchs et al. and the image quality of our algorithm is shown to be superior for the same number of iterations.

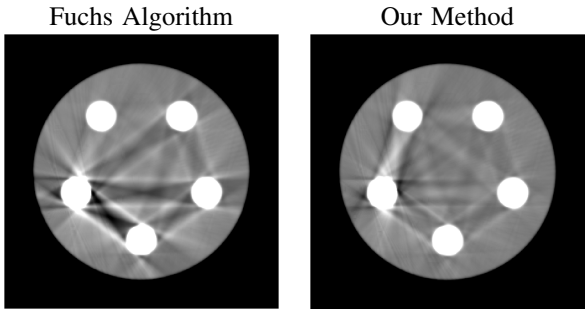

Fig. 3. Reconstructed images of the 6-material phantom after 2 iterations of each BHC algorithm. Window: [900, 1100] HU.

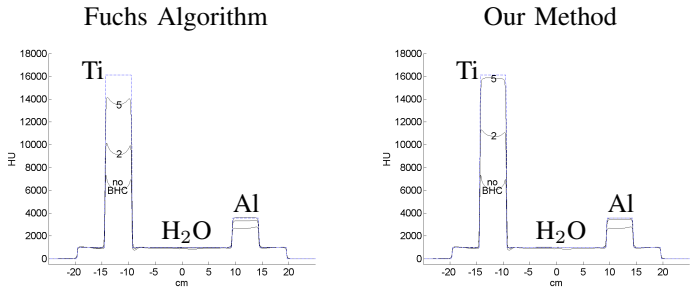

Fig. 4. Cross sectional plots through the reconstructed image of the 6-material phantom after two iterations of each BHC method. The numbers on the cross section plots represent the number of iterations of the BHC algorithm. The dashed line is the true cross section.

The *inner loop* of the BHC algorithm (the iteration in k) converges rapidly and can be computed in parallel because each measurement is processed independently. In our experiments nearly all data samples converged to within ten decimal places in three iterations or less. The computational complexity of our algorithm and the Fuchs algorithm is primarily driven by the number of forward and backprojection operations that are required per iteration. Our algorithm requires one forward projection and one backprojection per iteration while the Fuchs algorithm requires M (the number of materials in the model) forward projections and one backprojection per iteration. No forward or back projections are required for the first iteration of either algorithm, but one must perform an extra backprojection at the conclusion of both algorithms to produce an output image. Thus the number of forward and back projections required for N iterations is given by $2(N-1)+1$ and $(M+1)(N-1)+1$ for our algorithm and the Fuchs algorithm, respectively.

The main novel aspect of our algorithm is in the separation of the beam hardening model parameters, $c(\gamma, L)$, and the desired monochromatic sinogram, $p(L)$, described by equations (6, 7). This allows one to exactly determine the data that fits the given material model by computation of the inner loop in our algorithm. The outer loop updates the material model.

VIII. Acknowledgement

This work performed under the auspices of the U.S. Department of Energy by Lawrence Livermore National Laboratory under Contract DE-AC52-07NA27344, document release number LLNL-CONF-649613. The Imatron data was provided courtesy of the COE for Explosives ALERT at Northeastern University.

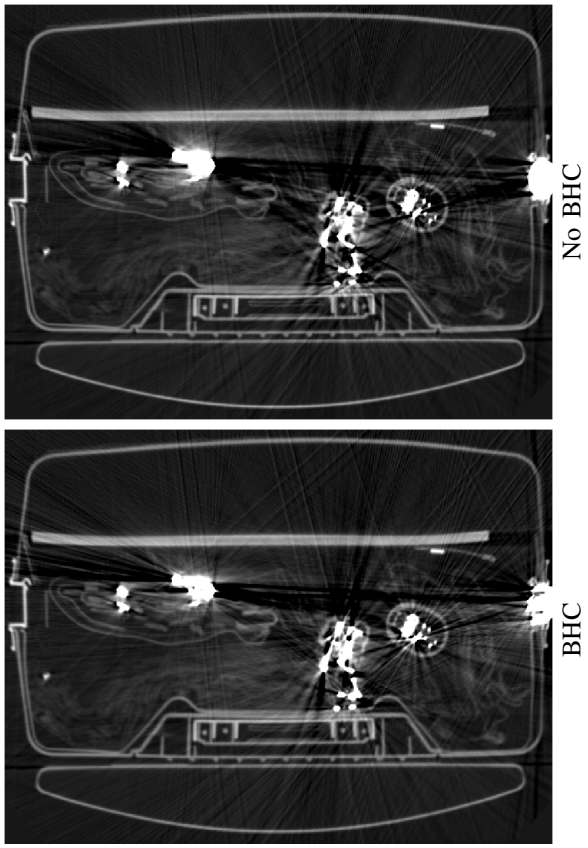

Fig. 5. Reconstructed images of luggage scanned on the Imatron EBCT scanner with display window [-200, 2000] HU.

References

[1] G. Herman and S. Trivedi. A comparative study of two postreconstruction beam hardening correction methods. *IEEE Trans. Med. Imaging*, 2:128–135, 1985.

[2] P. Joseph and C. Ruth. A method for simultaneous correction of spectrum hardening artifacts in ct images containing both bone and iodine. *Med. Phys.*, 24:1629–1634, 1997.

[3] T. Fuchs. Strahlaufhärtungskorrekturen in der computer-tomographie. *Ph.D. dissertation, Institut für Medizinische Physik, Friedrich-Alexander Universität*, 1998.

[4] J. Hsieh, R. Molthen, C. Dawson, and R. Johnson. An iterative approach to the beam hardening correction in cone beam ct. *Med. Phys.*, 27:23–29, 2000.

[5] Bruno De Man, Johan Nuyts, Patrick Dupont, Guy Marchal, and Paul Suetens. An iterative maximum-likelihood polychromatic algorithm for CT. *IEEE Trans. Med. Imag.*, 20:999–1008, 2001.

[6] I. Elbakri and J. Fessler. Segmentation-free statistical image reconstruction for polyenergetic x-ray computed tomography with experimental validation. *Phys. Med. Biol.*, 48:2453–2477, 2003.

[7] Marc Kachelrieß and Willi A. Kalender. Improving pet/ct attenuation correction with iterative ct beam hardening correction. *IEEE Nuclear Science Symposium Conference Record*, M04-5:1905–1909, 2005.

[8] G. Van Gompel, K. Van Slambrouck, M. Defrise, K. Batenburg, J. de-Mey, J. Sijbers, and J. Nuyts. Iterative correction of beam hardening artifacts in ct. *Med. Phys.*, 38:36–49, 2011.

[9] M.J. Berger, J.H. Hubbell, S.M. Seltzer, J. Chang, J.S. Coursey, R. Sukumar, D.S. Zucker, and K. Olsen. *XCOM: Photon Cross Section Database (version 1.5)*. National Institute of Standards and Technology, Gaithersburg, MD, 2010.

[10] G.G. Poludniowski. Calculation of x-ray spectra emerging from an x-ray tube. part ii. x-ray production and filtration in x-ray targets. *Med. Phys.*, 34:2175–2186, 2007.